Earth and Planetary Science Letters 549 (2020) 116497

Contents lists available at ScienceDirect

Earth and Planetary Science Letters

www.elsevier.com/locate/epsl

Evidence for early asteroidal collisions prior to 4.15 Ga from basaltic eucrite phosphate U–Pb chronology

Mizuho Koike [a,*], Yuji Sano [b,c], Naoto Takahata [b], Tsuyoshi Iizuka [d], Haruka Ono [d,e], Takashi Mikouchi [d,e]

[a] Earth and Planetary Systems Science Program, Graduate School of Advanced Science and Engineering, Hiroshima University, 1-3-1 Kagamiyama, Higashihiroshima-shi, Hiroshima, 739-8526, Japan
[b] Atmosphere and Ocean Research Institute, The University of Tokyo, Kashiwa, Chiba, 277-8564, Japan
[c] Institute of Surface-Earth System Science, Tianjin University, Nankai District, Tianjin, 300072, PR China
[d] Department of Earth and Planetary Science, The University of Tokyo, Bunkyo-ku, Tokyo, 113-0033, Japan
[e] The University Museum, The University of Tokyo, Bunkyo-ku, Tokyo, 113-0033, Japan

ARTICLE INFO

Article history:
Received 24 March 2020
Received in revised form 9 July 2020
Accepted 23 July 2020
Available online 26 August 2020
Editor: F. Moynier

Keywords:
eucrites
NanoSIMS
U-Pb chronology of phosphates
Vesta
early collisional history of asteroids

ABSTRACT

The late heavy bombardment (LHB) hypothesis, wherein the terrestrial planets are thought to have suffered intense collisions ca. 3.9 billion years ago, is under debate. Coupled with new dynamical calculations, re-examination of geochronological data seem to support an earlier solar system instability and a smooth monotonic decline in impacts, as opposed to a "cataclysm." To better understand this collisional history, records from the asteroidal meteorites are required. Here, we report a uranium–lead (U–Pb) chronological dataset for eucrite meteorites thought to originate from the asteroid 4 Vesta; this dataset indicates to a continuous history of collisions prior to 4.15 Ga. Our $^{207}Pb^*/^{206}Pb^*$ model ages of apatite [$Ca_5(PO_4)_3(F,Cl,OH)$] and merrillite [$Ca_9NaMg(PO_4)_7$] from three brecciated basaltic eucrites—Juvinas (4150.3 ± 11.6 million years ago (Ma); merrillite only), Camel Donga (disturbed around 4570–4370 Ma), and Stannern (4143.0 ± 12.5 Ma)—record multiple thermal metamorphic events during the period of ~4.4–4.15 Ga. We interpret this to mean that Vesta or the vestoid cluster underwent multiple impacts and moderate high-temperature reheating during this time. The ages of ~4.4–4.15 Ga are distinctly younger than the initial magmatic process on Vesta (>4.5 Ga) but are significantly older than a later "impact peak" based on some interpretations of ^{40}Ar–^{39}Ar chronologies (~3.9–3.5 Ga). The intense collisions prior to 4.15 Ga on Vesta are at odds with the conventional LHB hypothesis but not inconsistent with the much earlier bombardment and monotonic decline scenario. Different radiometric chronologies of the asteroid likely represent the different stages of a continual collisional process. Conversely, the model $^{207}Pb^*/^{206}Pb^*$ ages of apatite in the unbrecciated basaltic eucrite, Agoult, returned an age of 4524.8 ± 9.6 Ma. This may represent slow cooling from an earlier global reheating of the crust on Vesta at 4.55 Ga, as documented by other radiometric chronologies. The apatite in Juvinas recorded a coincident timing of 4516.9 ± 10.4 Ma, which could be due to either slow crustal cooling or impact.

1. Introduction

Geological and geochemical records of the Earth–Moon system seem to indicate a surge in the impact flux at ~3.9 billion years ago (Ga). Radiometric ages of multiple Apollo samples and lunar meteorites present a broad variation in ages with a peak at 3.9 Ga (e.g., Turner et al., 1973). Some studies interpret cratering ages of the large lunar basins as concentrated between ~4.0 Ga and 3.8 Ga (e.g., Stöffler and Ryder, 2001). The late heavy bombardment (LHB) hypothesis arose from such findings. Orbital migrations of Jupiter and the other giant planets, triggered by a massive early cometary disk in the trans-Neptunian region, may have caused the intense impacts within the inner solar system (Nice model; Gomes et al., 2005). If such planetary migrations occurred at 3.9 Ga, results like those from the LHB model might be observed. Chronological data from various asteroidal meteorites, however, cast doubt on this interpretation (Mojzsis et al., 2019). The alternative early instability scenario, where the earlier planetary migrations provoked inner solar system collisions that monotonically decreased over the

* Corresponding author.
E-mail address: mizuhokoike@hiroshima-u.ac.jp (M. Koike).

https://doi.org/10.1016/j.epsl.2020.116497
0012-821X/

next several hundreds of millions of years (Morbidelli et al., 2018; Clement et al., 2019), seems to better explain the present data. Recent geochronology-based re-examinations by Mojzsis et al. (2019) and Brasser et al. (2020) provide timing constraints showing that the terrestrial planets suffered the intense bombardments at or before 4.48 Ga. Because most records on the terrestrial planets were overwritten by later internal and external processes, geochronologies of asteroids are valuable hints for understanding the ancient collisional history.

Asteroid 4 Vesta is one of the largest rocky bodies in the main asteroid belt. The genetic linkage between Vesta (and its spectral resemblances, V-type asteroids) and howardite–eucrite–diogenite (HED) meteorites has been advocated based on petrographic studies of meteorites and telescopic observations of the asteroid since the 1960–1970s (McCord et al., 1970). Direct observations by the NASA Dawn Mission in 2012 further support the Vesta–HED relationship (Russell et al., 2012; McSween et al., 2013). As members of the HED clan, eucrites are basaltic or gabbroic crustal rocks primarily composed of low-Ca pyroxene, plagioclase, and minor amounts of silica minerals, sulfides, oxides, Ca phosphates, and rare zircons (e.g., Palme et al., 1988; Takeda and Graham, 1991; Metzler et al., 1995; and Yamaguchi et al., 1996, 2009). Based on short-lived radiometric chronometers, previous studies have shown that the initial crystallization of basaltic eucrites occurred within a few million years after the formation of the solar system (e.g., Lugmair and Shukolyukov, 1998; Touboul et al., 2015; Hublet et al., 2017). Most of the basaltic eucrites subsequently experienced high-temperature (~900 °C) annealing (Haba et al., 2014; Iizuka et al., 2015; Liao and Hsu, 2017). The U–Pb and Hf–W ages of zircons in the basaltic eucrites vary from as old as ~4563–4565 million years ago (Ma) to 4530 Ma (Ireland and Bukovanská, 1992; Misawa et al., 2005; Srinivasan et al., 2007; Zhou et al., 2013; Roszjar et al., 2016; Liao and Hsu, 2017; Liao et al., 2019), with a weighted mean U–Pb age of 4554 ± 2 Ma (Iizuka et al., 2015). The eucritic zircons are considered to have crystallized during the initial crust formation and/or the prolonged thermal processes on Vesta. An old zircon with an age of 4563 ± 15 Ma has also been reported in a mesosiderite (Ireland and Wlotzka, 1992), another meteoritical group that is expected to have a common origin with the HEDs (i.e., Vesta). After a suite of the early processes, most eucrites experienced complicated geologic events including (multiple cycles of) impact brecciation, reheating, and partial remelting. The ^{40}Ar–^{39}Ar dating of various eucrites exhibits a large age variation from ~4.5 Ga to 3.5 Ga (review by Bogard, 2011). Recent re-assessments of the ^{40}Ar–^{39}Ar plateau ages indicate two groups: an earlier group with ^{40}Ar–^{39}Ar plateau ages at ~4.50 Ga and a later group with ages at ~3.85–3.47 Ga (Kennedy et al., 2013, 2019). The earlier group may be associated with a large impact on Vesta that resulted in the formation of an ancient basin (possibly Veneneia) (Kennedy et al., 2013, 2019). The timing of this basin-forming or related cataclysmic impact on Vesta has also been dated at 4.52–4.53 Ga by other chronological studies (Hopkins et al., 2015; Haba et al., 2019). The later Ar-plateau ages, conversely, are interpreted either as clustering impacts during ~3.85–3.47 Ga or as an "end-tail" of ancient continuous collisions (Kennedy et al., 2019).

The U–Pb chronology of Ca phosphates, such as apatite [$Ca_5(PO_4)_3(F,Cl,OH)$], is useful. Closure temperatures for radiometric chronometers are known to be quite high for the U–Pb system in zircon, "moderately high" for the U–Pb in apatite, and considerably lower for the K–Ar system in plagioclase (respectively ~900 °C, ~450 °C, and ~300 °C, assuming typical mineral sizes and slow cooling of 1–100 °C/Myr; Cherniak and Watson, 2000; Cherniak et al., 1991; Cassata et al., 2009). Thus, the U–Pb system in apatite provides a record of "moderately high-temperature" events that were likely missed or overwritten in other radiometric systems. Another Ca phosphate, merrillite [$Ca_9NaMg(PO_4)_7$], often provides a similar U–Pb chronology, although its closure temperature remains to be experimentally determined. The U–Pb age of apatite in a brecciated basaltic eucrite, Béréba, was reported at 4.2 Ga (Zhou et al., 2011); this age was originally interpreted as the beginning of LHB on the asteroid. Liao and Hsu (2017) reported the similar U–Pb ages of 4.2–4.1 Ga from apatite and merrillite in a newly found eucritic impact-melt breccia, Northwest Africa (NWA) 8009. According to their mineralogical and geochemical study by Liao and Hsu (2017), NWA 8009 experienced an abnormally severe impact compared to other eucrites, with a peak pressure of ~50–60 GPa and a temperature of ~1160–1200 °C. Conversely, the apatite U–Pb age of another unbrecciated eucrite, NWA 6594, recorded an earlier event at 4523 ± 2 Ma (Liao et al., 2019). Liao et al. (2019) attribute this age to a large cataclysmic impact on Vesta, as inferred from other chronologies (Kennedy et al., 2013, 2019; Hopkins et al., 2015; Haba et al., 2019). By extending this line of reasoning to multiple eucrites, the thermal and collisional history of Vesta can be determined and, by implication, that of the other asteroid belt bodies. Here, we present a new U–Pb dataset for several eucritic phosphates, which indicates that their parent bodies suffered complicated thermal/impact metamorphism at a very early stage.

2. Sample descriptions

Four basaltic eucrites (Juvinas, Camel Donga, Stannern, and Agoult) with an anomalous basaltic achondrite, Ibitira, were studied in this paper. Of the five, three (Juvinas, Camel Donga, and Stannern) are breccias, and the other two (Agoult and Ibitira) are unbrecciated granulites. Brief descriptions of the meteorites are given in the following subsections. The details are summarized in Table 1.

2.1. Juvinas

Juvinas is known to have fallen in France in 1821. It is composed of various igneous clasts, a porous matrix, and recrystallized areas (Metzler et al., 1995). According to the metamorphic classification of basaltic eucrites proposed by Takeda and Graham (1991), the chemically equilibrated pyroxenes in Juvinas indicate a thermal metamorphic grade of 5 (1: pristine, 6: most metamorphosed). Various chronologies of Juvinas exhibit large variations, reflecting its extremely complicated metamorphic history (Table 1). The ^{207}Pb–^{206}Pb age of its zircons has been reported at ~4560 Ma (Bukovanska and Ireland, 1993) and 4545 ± 15 Ma (Zhou et al., 2013). These values are consistent with the ^{182}Hf–^{182}W isochron age of 4546 ± 3 Ma for the whole rock and its silicate fractions (anchored by the D'Orbigny angrite; Touboul et al., 2015). Conversely, the ^{207}Pb–^{206}Pb isochron of the Juvinas silicates indicates a significantly younger age of 4320 ± 1.7 Ma (Galer and Lugmair, 1996). Its ^{40}Ar–^{39}Ar age was disturbed much later at ~4.0 Ga (Kaneoka et al., 1995).

2.2. Camel Donga

Camel Donga was found in Western Australia in 1984. This meteorite is a severely metamorphosed polymict breccia (Warren et al., 2017; Ono et al., 2018). Its highly equilibrated pyroxene indicates severe thermal metamorphism (Palme et al., 1988; Metzler et al., 1995). A unique characteristic of Camel Donga is its anomalously high abundances of secondary metallic Fe (up to 2 wt%), which is thought to be the result of decomposition of initial Fe sulfides and silicates during post-crystallization reheating (Palme et al., 1988; Warren et al., 2017). Mineralogical and chronological studies of Camel Donga also indicate its complicated metamorphism (Table 1). The Al–Mg short-lived radiometric system in this

Table 1
Summary of the studied meteorites.

	Juvinas	Camel Donga	Stannern	Agoult	Ibitira
mineralogy & petrology					
fall / found	fall	find	fall	find	fall
parent body	Vesta	Vesta	Vesta	Vesta	unknown
brecciation	monomict breccia	polymict breccia	monomict breccia	monomict breccia	unbrecciated
	equilibration of pyroxenes (type 5[a])	equilibration of pyroxenes (type 5[a])	equilibration of pyroxenes with remnant zoning (type 4[a]);	fine-grained granulite (type 5);	fine-grained hornfelsic (type 5[e]);
thermal metamorphism	recrystallization of mesostasis; euhedral tridymite crystal[b]	recrystallization of mesostasis[b] secondary metallic Fe[c]	recrystallization of mesostasis[b]	recrystallization and exsolution of secondary minerals[d]	recrystallization of mesostasis; euhedral tridymite crystal[f]
Selected chronologies (Ma)					
Pb-Pb (zircon)[g]	4545 ± 15	4531 ± 10	4550 ± 10	4554.5 ± 2.0	Not reported
Pb-Pb (silicates or oxides)[h]	4320 ± 1.7	4515.43 ± 0.42 Ma	4128 ± 16	4532.29 ± 0.87 Ma	4556.75 ± 0.57
Pb-Pb (phosphates)[i]	apt: 4516.9 ± 10.4 mer: 4150.3 ± 11.6	4491.4 ± 13.5 (young outlier: 4372 +26/−27)	4143.0 ± 12.5 (old outlier: 4202 ± 24/−25)	4524.8 ± 9.7	4552.0 ± 8.8
Ar-Ar (stepwise heating of whole rock or plagioclase)[j]	~4100–4000 Ma (disturbed)	3749 ± 25 Ma	~4200–3800 Ma (disturbed)	4496 ± 8 Ma	4487 ± 15

The data are from [a] Takeda and Graham (1991); [b] Metzler et al. (1995); [c] Palme et al. (1988); [d] Yamaguchi et al. (2009); [e] Miyamoto et al. (2001); [f] Yamaguchi et al. (1996); [g] Ireland and Bukovanská (1992), Zhou et al. (2013), Iizuka et al. (2015); [h] Galer and Lugmair (1996), Tera et al. (1997), Iizuka et al. (2014, 2019); [i] *the mean model* $^{207}Pb^*/^{206}Pb^*$ *ages from this study*; [j] Kaneoka et al. (1995), Bogard and Garrison (1995); Iizuka et al. (2019), and Kennedy et al. (2019).

eucrite recorded early crystallization at 4564.31 $+0.98/-3.48$ Ma (Hublet et al., 2017). Its zircon $^{207}Pb/^{206}Pb$ age is 4531 ± 10 Ma (Zhou et al., 2013), resolvably younger than those of the other basaltic eucrites with mean values of 4555 Ma (Misawa et al., 2005; Zhou et al., 2013; Iizuka et al., 2015). Its oxide ^{207}Pb–^{206}Pb age has been determined to be 4515.43 ± 0.42 Ma (Iizuka et al., 2019), slightly younger than its zircon age. Meanwhile, its plagioclase recorded a significantly younger ^{40}Ar–^{39}Ar age of 3750 Ma (Kennedy et al., 2013; Iizuka et al., 2019).

2.3. Stannern

Stannern is a monomict brecciated eucrite that fell in the Czech Lands in 1801. Compared to Juvinas and Camel Donga, its pyroxene chemistry and textural properties exhibit weak thermal effects, suggesting a metamorphic grade of 4 (Takeda and Graham, 1991; Metzler et al., 1995). Chronological studies of Stannern have revealed an old crystallization age of 4564 ± 2 Ma (Hf–W isochron age; Touboul et al., 2015) and multiple later metamorphic events. Its slightly younger zircon ^{207}Pb–^{206}Pb age has been reported at 4550 ± 10 Ma (Ireland and Bukovanská, 1992). The U–Pb and K–Ar systems in its silicates were severely disturbed (Tera et al., 1997; Kennedy et al., 2019).

2.4. Agoult

Agoult is a monomict unbrecciated basaltic eucrite that was found in Morocco in 2000. It is composed of fine-grained granulitic textures with 120° triple junctions, indicating significant recrystallization (Yamaguchi et al., 2009). Its pyroxenes are chemically well equilibrated between homogeneous low-Ca pyroxene and augite. The trace element patterns of this meteorite are similar to those of the Main Group–Nuevo Laredo trend eucrites, even though Agoult is thought to have undergone partial melting during thermal metamorphism (Yamaguchi et al., 2009). Both U–Pb and K–Ar systems in Agoult have preserved ancient thermal processes. The ^{207}Pb–^{206}Pb isochron ages of zircons and oxides in Agoult are dated at 4554.5 ± 2.0 Ma and 4532.29 ± 0.87 Ma (Iizuka et al., 2015, 2019), respectively. Its plagioclase presents a young ^{40}Ar–^{39}Ar plateau age at 4494 ± 9 Ma (Iizuka et al., 2019). Such chronological variations may be associated with slow cooling. Iizuka et al. (2019) estimated the cooling rate of the Agoult host rock at 11 ± 2 °C/Myr after thermal metamorphism at 4554.5 Ma.

2.5. Ibitira

Ibitira was found in Brazil in 1957. The mineralogical and chemical features of Ibitira are indistinguishable from those of recrystallized basaltic eucrites (Yamaguchi et al., 1996). However, its several unique features, such as vesicle-rich textures and alkali element depletions, suggest that Ibitira came from a parent body other than Vesta. The oxygen three-isotopic composition of Ibitira is reported to be $\Delta^{17}O = -0.07$ (Scott et al., 2009), significantly higher than the known eucrite fractionation line ($\Delta^{17}O = -0.239 \pm 0.007‰$; Greenwood et al., 2005). The pyroxenes in Ibitira were thermally well equilibrated, suggesting a metamorphic grade of 5 (Takeda and Graham, 1991; Miyamoto et al., 2001). Similar to Agoult, the chronologies of Ibitira indicate ancient thermal processes. Short-lived Mn–Cr systems have indicated an age of 4556 ± 3 Ma (Lugmair and Shukolyukov, 1998). Its identical pyroxene ^{207}Pb–^{206}Pb age has been precisely determined at 4556.75 ± 0.57 Ma (Iizuka et al., 2014). Its ^{40}Ar–^{39}Ar age has been reported at 4,487 ± 15 Ma (Bogard and Garrison, 1995), which overlaps the ages of some unbrecciated eucrites (4,480 ± 20 Ma; Bogard and Garrison, 2003).

3. Methods: NanoSIMS U–Pb dating

Polished thick sections of the five meteorites were carbon-coated and observed using SEM-EDS and EPMA to locate apatite and/or merrillite minerals with analyzable grain sizes (≥10 μm) and study their petrological features. After NanoSIMS dating, the major element compositions of these phosphates were analyzed using a JXA-8530F (JEOL) at the Department of Earth and Planetary Science, University of Tokyo, Japan. The mineral phases of adjacent silica minerals were also observed following the NanoSIMS analyses using a Raman spectrometer (JASCO NRS-1000) at the National Institute of Polar Research, Japan. The detailed conditions and results of the observational studies are described in the supplementary information.

All samples were slightly re-polished (<~0.3 μm) after the initial SEM-EDS observations and then gold coated and baked at ~100 °C in the NanoSIMS air-lock system prior to the isotopic

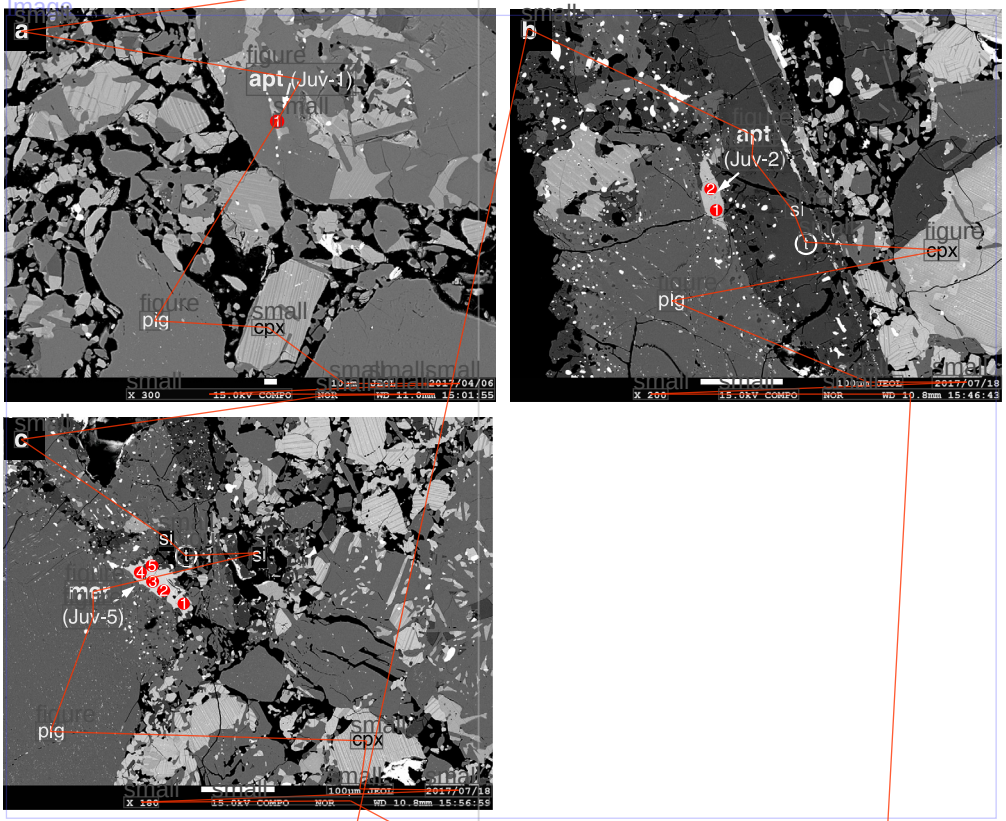

Fig. 1. Back-scattered electron images of the Juvinas phosphates: (a) apatite in the lithic clast (apt #1) and (b, c) apatite and merrillite in the fine-grained matrix areas. Labels attached to the individual phosphates correspond to Tables S1 and S2. Red-filled circles with numbers indicate the NanoSIMS spots. Opened circles with "t" (tridymite) or "q" (quartz) depict the Raman spots. The abbreviations are apt: apatite, mer: merrillite, cpx: pigeonite and augite, plg: plagioclase, and si: silica minerals. (For interpretation of the colors in the figure(s), the reader is referred to the web version of this article.)

analyses. Both ^{238}U–^{206}Pb dating and ^{207}Pb–^{206}Pb dating were conducted using a NanoSIMS 50 (Ametek Inc.) at Atmosphere and Ocean Research Institute, University of Tokyo, Japan. The detailed analytical protocols and calibration methods are given in Takahata et al. (2008) and Koike et al. (2014). A 2-nA O^- beam was focused with a spot size of approximately 10 µm. To obtain the ^{238}U–^{206}Pb age, secondary ions of $^{31}P^+$, $^{43}Ca^+$, $^{204}Pb^+$, $^{206}Pb^+$, $^{238}U^{16}O^+$, and $^{238}U^{16}O_2^+$ were simultaneously collected for 600 s per spot using the NanoSIMS multi-collectors. Then, in the magnetic peak jumping mode, the secondary ions of $^{204}Pb^+$, $^{206}Pb^+$, and $^{207}Pb^+$ were measured at the same spot for ~1 h to determine the ^{207}Pb–^{206}Pb age. A natural apatite standard from Canada (called "PRAP" in Sano et al., 1999) was used to calibrate the measured $^{238}U/^{206}Pb$ ratios in the $^{206}Pb^+/^{238}U^{16}O^+$–$^{238}U^{16}O_2^+/^{238}U^{16}O^+$ diagram. The ^{238}U–^{206}Pb and ^{207}Pb–^{206}Pb isochron ages were calculated using Isoplot software (Ludwig, 2012). The isochron ages were calculated for the individual meteorites, assuming that all phosphates in one meteorite (except for Juvinas, discussed later) recorded the same history. The model $^{207}Pb^*/^{206}Pb^*$ ages were calculated for the individual data, which provide *in-situ* thermal histories for individual analyzed areas. We assumed an initial $^{207/206/204}Pb$ composition (same to the Canyon Diablo troilite) and a specific $^{238}U/^{235}U$ ratio for the model $^{207}Pb^*/^{206}Pb^*$ calculations, which does not affect our results and discussion. For details concerning the age calculations, see the supplementary information.

4. Results

4.1. U–Pb chronology of phosphates in the brecciated eucrites

In Juvinas, several anhedral grains of F-rich apatite and merrillite were found in both lithic clasts and around the fine-grained high-porosity matrix (Fig. 1). The matrix contains numerous opaque minerals with size variations from submicron to ~10 µm. A large elongated silica grain composed of quartz and tridymite, with a size of 100 µm (wide) × ~3 mm (long), appears abruptly between the coarse-grained lithic clasts and the fine-grained porous matrix (for details concerning the silica minerals, see the supplementary information). These silica polymorphs provide additional information about thermal and metamorphic histories (Liao et al., 2019). All phosphates in the matrix areas are located adjacent to the quartz–tridymite grain. The apatite in the coarse-grained lithic areas (Fig. 1a) does not exhibit such a relationship. Three apatite grains, two from the matrix and one from the lithic clast, with four spot data, define a ^{207}Pb–^{206}Pb isochron age of 4552 ± 85 Ma (mean square weighted deviation (MSWD) = 0.48). Hereafter, the age uncertainties are at the 95% confidence level. The model $^{207}Pb^*/^{206}Pb^*$ ages were calculated to be ~4630–4485 Ma, with a weighted mean of 4516.9 ± 10.4 Ma (Fig. 4). Their ^{238}U–^{206}Pb isochron age was poorly determined at 5037 ± 480 Ma (MSWD = 0.10). The large uncertainty in this age is primarily because most data points have indistinguishable $^{204}Pb/^{206}Pb$ ratios, which resulted in a small MSWD value of 0.1 (for details, see the supplementary information). Conversely, the four merrillite grains with eight data define a ^{207}Pb–^{206}Pb isochron age as young as 4200 ± 49 Ma (MSWD = 0.59). Their model $^{207}Pb^*/^{206}Pb^*$ ages range between ~4170 Ma and 4080 Ma with a weighted mean of 4150.3 ± 11.6 Ma (Fig. 4). Their ^{238}U–^{206}Pb isochron ages could not be determined. Detailed results of all the ^{238}U–^{206}Pb and ^{207}Pb–^{206}Pb isochrons are presented in Figs. S7–S12. All the isotopic data are presented in Table S2.

In Camel Donga, several anhedral grains of F-rich apatite (~10–200 µm) were found in coarse-grained lithic clasts and the granulitic recrystallized matrix (Fig. 2). The nearby silica mineral

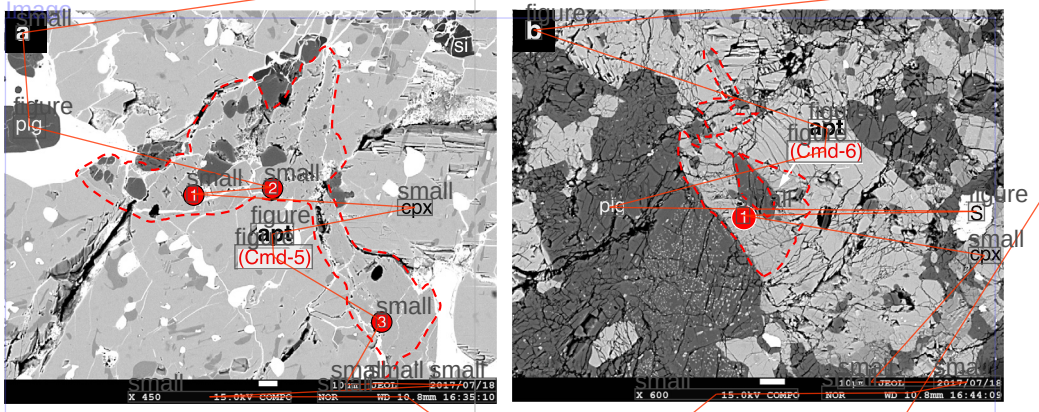

Fig. 2. Back-scattered electron images of the Camel Donga phosphates in (a) the recrystallized matrix area and (b) the lithic clast. Labels attached to the individual phosphates correspond to Tables S1 and S2. Red-filled circles with numbers indicate the NanoSIMS spots. The abbreviations are apt: apatite, cpx: pigeonite and augite, plg: plagioclase, si: silica minerals, and S: iron sulfide.

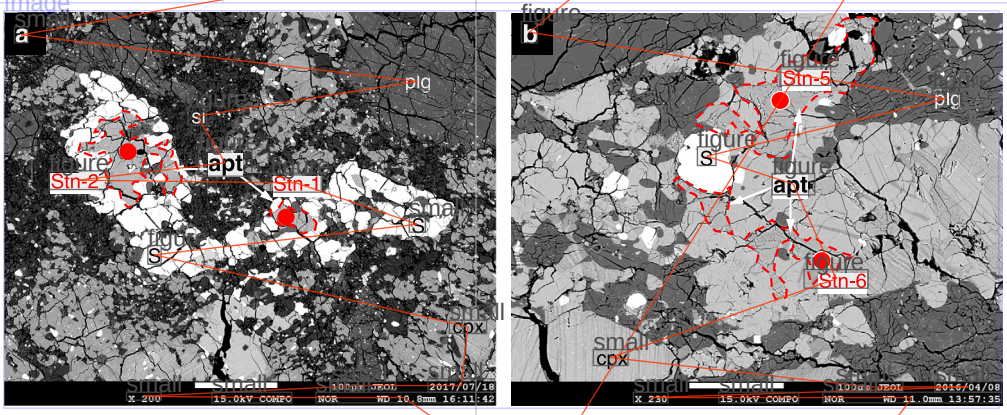

Fig. 3. Back-scattered electron images of the Stannern phosphates in (a) the re-crystallized matrix area and (b) the lithic clast. Labels attached to the individual phosphates correspond to Tables S1 and S2. Red-filled circles indicate the NanoSIMS spots. The abbreviations are apt: apatite, cpx: pigeonite and augite, plg: plagioclase, si: silica minerals, and S: iron sulfide.

phases are quartz, monoclinic tridymite, and pseudo-orthorhombic tridymite (Ono et al., 2018). The ^{238}U–^{206}Pb and ^{207}Pb–^{206}Pb isochron ages were calculated using six apatite grains with eight spot data, giving ages of 4222 ± 430 Ma (MSWD = 1.12) and 4465 ± 82 Ma (MSWD = 5.0), respectively. The large MSWD value of 5.0 means that the isotopic data are highly scattered. The model $^{207}Pb^*/^{206}Pb^*$ ages vary between ~4570 Ma and 4370 Ma. Their weighted mean value was calculated at 4491.4 ± 13.5 Ma (Fig. 4), except for the youngest outlier, which had an age of 4372 +26/−27 Ma (Cmd-4). There is no apparent correlation between the textural/chemical properties of the individual apatite grains and their $^{207}Pb^*/^{206}Pb^*$ ages.

Stannern also contains several F-rich apatite and merrillite grains in igneous lithic clasts and in the granulitic recrystallized matrix (Fig. 3). Apatite grains in the granulitic areas appear as an intergrowth with ilmenite, plagioclase, and silica-rich mesostasis (Fig. 3). Numerous fractures intersect both the granulitic areas and the surrounding igneous clasts. The apatite and merrillite grains in the igneous clasts are anhedral and highly fractured and are adjacent to equilibrated pyroxene, plagioclase, and isolated ilmenite (Fig. 3). The six apatite grains and one merrillite grain yielded a young ^{238}U–^{206}Pb isochron age of 3975 ± 110 Ma (MSWD = 0.27) and a ^{207}Pb–^{206}Pb isochron age of 4134 ± 47 Ma (MSWD = 5.3). The high MSWD value indicates that the U–Pb system in the Stannern phosphates has been disturbed. The model $^{207}Pb^*/^{206}Pb^*$ ages vary from ~4,270 Ma to 4,080 Ma. Their weighted mean value is 4143.0 ± 12.5 Ma (Fig. 4), except for the oldest outlier (Stn-5; 4202 +24/−25 Ma).

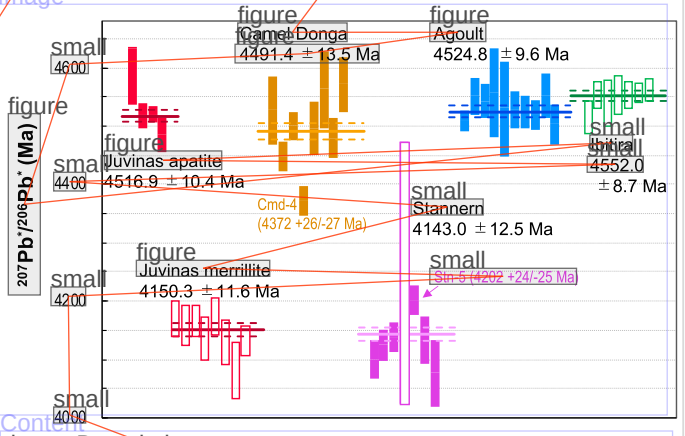

Fig. 4. Model $^{207}Pb^*/^{206}Pb^*$ ages of all the analyzed phosphates. The filled symbols indicate apatite ages with two-sigma errors, whereas the opened symbols indicate merrillite ages. The horizontal lines represent the weighted mean values of the individual meteorites. The two outliers, Cmd-4 ($^{207}Pb^*/^{206}Pb^*$ age at 4372 +26/−27 Ma) and Stn-5 ($^{207}Pb^*/^{206}Pb^*$ age at 4202 +24/−25 Ma), were excluded from the weighted mean calculations.

4.2. U–Pb chronology of phosphates in the unbrecciated achondrites

In Agoult, euhedral to rounded grains of F-rich apatite with sizes of 10–100 μm were observed homogeneously throughout the studied section (Fig. S4). Their U–Pb age can be determined more precisely compared to those of the other brecciated eucrites. The seven grains with 10 spot analyses yielded a ^{238}U–^{206}Pb isochron

age of 4350 ± 290 Ma (MSWD = 1.2) and a ^{207}Pb–^{206}Pb isochron age of 4530 ± 17 Ma (MSWD = 2.0). The model $^{207}Pb^*/^{206}Pb^*$ ages are between ~4560 Ma and 4504 Ma, with a weighted mean of 4524.8 ± 9.7 Ma (Fig. 4).

Ibitira is characterized by numerous spherical vesicles with sizes of 100–500 μm in its unbrecciated recrystallized area. On the wall of the vesicle, a ~150 μm round-shaped grain of merrillite was identified (Fig. S5). Smaller grains (~20 μm) of merrillite were also found in its igneous textures. The five merrillite grains with seven spot analyses did not define a ^{238}U–^{206}Pb isochron or ^{207}Pb–^{206}Pb isochron age with meaningful precision, primarily because of the overlapping of the data. The model $^{207}Pb^*/^{206}Pb^*$ age was calculated at 4563–4515 Ma, with a weighted mean of 4552.0 ± 8.8 Ma (Fig. 4).

5. Discussion

5.1. Two ages in Juvinas: older apatite and younger merrillite

Only Juvinas presents two distinctly different ages for apatite and merrillite. The model $^{207}Pb^*/^{206}Pb^*$ ages are 4516.9 ± 10.4 Ma for the apatite and 4150.3 ± 11.6 Ma for the merrillite (Fig. 4). Most apatite (except for Juv-1 in Fig. 1a) and all merrillite grains are located in a close area, even though they recorded completely different timings. One possible explanation is that the U–Pb system in merrillite can more readily be reset than that in apatite so that only merrillite records the 4150-Ma event. Although we know the U–Pb closure temperature of apatite (discussed later), unfortunately, there is no available information for merrillite at this moment. Previous SIMS U–Pb studies have not found such age differences between meteoritical apatite and merrillite (Sano et al., 2000; Terada and Sano, 2002). It is likely that the U–Pb systems in apatite and merrillite record the same events in regular cases. Another, more plausible case is that the reheating temperature in the 4,150-Ma event was heterogeneous and that it locally reached higher temperatures. The relationship between the apatite/merrillite and the adjacent silica polymorphs supports this interpretation. Tridymite is a high-temperature silica phase (stable at 870–1470 °C under 1 atm; Fenner, 1913). The tridymite in Juvinas has a smooth surface and euhedral to subhedral shapes (Fig. 1), suggesting that it recrystallized from primary mesostasis (or its partial melt) during a high temperature reheating (>870 °C) and subsequent rapid cooling process. We assume this event to be identical to the merrillite $^{207}Pb^*/^{206}Pb^*$ age, because all of the merrillite grains are located close to the tridymite. It is likely that they suffered the local heterogeneous thermal metamorphism at 4150 Ma. Similar metamorphic origins of tridymite have been suggested for several basaltic eucrites (Yamaguchi et al., 1996; Liao et al., 2019). Conversely, the porous and anhedral quartz may be a relic of igneous mesostasis, consistent with observations of other basaltic eucrites (Fig. 1; Liao et al. (2019) and references therein). Considering that the apatite is located close to the mesostasis quartz, as well as in the lithic clast, the apatite should be an igneous relic mineral.

5.2. Brecciated eucrites are consistent with a continual collisional history

What do the two ages found in Juvinas mean? Both the apatite (~4520 Ma) and the merrillite (~4150 Ma) in Juvinas are significantly younger than the crystallization age of Juvinas whole rock dated by the Mn–Cr system at 4562.5 ± 1.0 Ma (Lugmair and Shukolyukov, 1998). The U–Pb age of the Juvinas zircon recorded a thermal event at 4545 ± 15 Ma (Zhou et al., 2013), consistent with the ubiquitous crustal metamorphism of Vesta at 4554.5 ± 2.0 Ma (Iizuka et al., 2015). The 4520-Ma Juvinas apatite is expected to have recorded either a slow cooling process subsequent to the 4554-Ma crustal metamorphism similar to the case of the Agoult apatite (discussed in the following subsection), or independent impact reheating similar to the previous NWA 6594 apatite (Pb-Pb age of 4523 ± 2 Ma; Liao et al., 2019). Conversely, the 4150-Ma merrillite accompanied by tridymite may represent the timing of an intense impact reheating event. The U–Pb systems in the Juvinas pyroxene and plagioclase were also severely disturbed (Galer and Lugmair, 1996). Their ^{207}Pb–^{206}Pb mineral isochron age was reported at 4320.9 ± 1.7 Ma (Galer and Lugmair, 1996), which may be the result of an incomplete U–Pb reset at a later reheating event (i.e., the 4150-Ma event). The K–Ar system was further disturbed (the ^{40}Ar–^{39}Ar age around ~4100–4000 Ma; Kaneoka et al., 1995), implying a weaker event. To summarize, Juvinas likely suffered severe impacts at 4320–4150 Ma and weaker reheating at ~4000 Ma. The metamorphic history of Juvinas can be explained as follows: (i) original crystallization at 4563 Ma, (ii) thermal crustal metamorphism and formation of secondary zircons at ~4550 Ma, (iii) closure/reset of the apatite U–Pb system at ~4520 Ma through slow cooling or impact reheating, (iv) a later reset of the U–Pb system in merrillite at ~4150 Ma through impact reheating, and (v) a final disturbance of the K–Ar system at ~4000 Ma possibly due to a weaker impact.

The U–Pb systems in the Camel Donga apatite are severely disturbed. Even though the mean model $^{207}Pb^*/^{206}Pb^*$ age was determined to be 4491.4 ± 13.5 Ma, the youngest outlier (Cmd-4) recorded an age of 4372 ± 26 Ma (Fig. 4). No apparent correlation was observed between the $^{207}Pb^*/^{206}Pb^*$ ages and the textural properties of the individual apatite grains (Figs. 2 and S2). The mean age of ~4490 Ma is ~30 Myr younger than the $^{207}Pb^*/^{206}Pb^*$ age of the Agoult apatite (4525 Ma; Fig. 4). This time lag of ~30 Myr between Camel Donga and Agoult is similar to the U–Pb systems in their zircons (Table 1: Camel Donga, 4531 ± 10 Ma; Agoult, 4454.5 ± 2.0 Ma; Zhou et al., 2013; Iizuka et al., 2015) and oxides (Camel Donga, 4,515.43 ± 0.42 Ma; Agoult, 4532.39 ± 0.87 Ma; Iizuka et al., 2019). The 4490-Ma apatite is consistent with a previous interpretation that Camel Donga resided in a distinct region on the parent body and underwent the thermal metamorphism at depth the crust ~20 Myr later than the other eucrites (Iizuka et al., 2019). In addition, the presence of young apatite at 4372 ± 26 Ma indicates that there was a distinct reheating event at ~4370 Ma, which caused an incomplete disturbance of the U–Pb system. Conversely, the ^{40}Ar–^{39}Ar age in the Camel Donga plagioclase was completely reset at 3749 ± 25 Ma because of an independent impact (Iizuka et al., 2019). This last event at ~3750 Ma caused diffusion and brecciation of the host rock, even though the reheating temperature was not high enough to reset the U–Pb system in the apatite. To summarize, the metamorphic history of Camel Donga can be described as follows: (i) initial crystallization at 4564 Ma (Hublet et al., 2017), (ii) high-temperature thermal metamorphism in the crust at 4530 Ma, (iii) subsequent slow cooling until 4490 Ma, (iv) an additional impact causing an incomplete disturbance of the apatite U–Pb system at 4370 Ma, and (v) final impact brecciation at 3750 Ma, where only the K–Ar system was reset.

The mean $^{207}Pb^*/^{206}Pb^*$ age of the Stannern phosphates also recorded young metamorphism at 4143.0 ± 12.5 Ma (Fig. 4), suggesting that they experienced severe impact reheating at this time. In contrast to Juvinas, both the apatite and merrillite in Stannern yielded identical ages. This may be because the host rock of Stannern was reheated more homogeneously to the U–Pb reset temperature. According to geochemical studies of the trace incompatible element trends, the geological backgrounds of Stannern and Juvinas should be different, which means that they resided at different locations on Vesta (e.g., Barrat et al., 2007). Their identical reheating ages of ~4150 Ma indicate that there were two (or more) impact events on Vesta during this period, where the re-

heating temperature was high enough to reset the U–Pb system in the phosphates (≥ ~590–1000 °C; discussed later) but inadequate to reset that of the zircon. Moreover, the ^{207}Pb–^{206}Pb age of the Stannern pyroxene and plagioclase also recorded this event at 4128 ± 16 Ma (Tera et al., 1997). The Stannern ^{40}Ar–^{39}Ar age was disturbed at ~4200–3800 Ma and did not present a plateau age (Kunz et al., 1995; Kennedy et al., 2019). Conversely, several radiometric chronologies place the early crystallization of Stannern at 4563 Ma (e.g., Lugmair and Shukolyukov, 1998; Touboul et al., 2015). Its zircon ^{207}Pb–^{206}Pb age recorded early thermal metamorphism at 4550 ± 10 Ma (Ireland and Bukovanská, 1992). Therefore, the metamorphic history of Stannern can be summarized as follows: (i) ancient crystallization at 4563 Ma, (ii) thermal crustal metamorphism at 4550 Ma, (iii) a reset of the U–Pb system in the phosphates and silicates at ~4140 Ma through intense impact reheating, and (iv) a subsequent weaker impact at sometime between ~4500 Ma and ~3600 Ma, where the K–Ar chronometer was disturbed. Events (iii) and (iv) may indicate the same event.

5.3. Unbrecciated achondrites represent the initial cooling of asteroids

The U–Pb systems in the unbrecciated samples, Agoult and Ibitira, recorded significantly ancient events prior to 4.5 Ga. The model ^{207}Pb*/^{206}Pb* age of the Agoult apatite, 4524.8 ± 9.6 Ma (Fig. 4), is identical to or slightly younger than the ^{207}Pb–^{206}Pb age of its oxide fraction (4532.39 ± 0.87 Ma) and is significantly younger than that of the zircon (4554.5 ± 2.0 Ma; Iizuka et al., 2015, 2019). The age differences between the different minerals may reflect the slow cooling of the Agoult host rock. It is likely that the rock was buried within the crust after its original crystallization and was subsequently heated by the hot interior of Vesta (Iizuka et al., 2019). The original internal heat source, a short-lived radionuclide (^{26}Al; $t_{1/2}$ ~0.7 Myr), had mostly decayed by this time (~4555–4525 Ma). However, according to a thermo-chemical evolution calculation (Neumann et al., 2014), the interior of the mantle of Vesta likely maintained a high temperature for >100 Myr after differentiation. The recrystallized textures of Agoult, with no apparent evidence of impact brecciation, further support this hypothesis of crustal thermal metamorphism. The ^{40}Ar–^{39}Ar plateau age of the Agoult plagioclase at 4496 ± 8 Ma (Iizuka et al., 2019) recorded the end of its subsequent slow cooling. To summarize, Agoult has the following thermal history: (i) ancient crystallization at >4560 Ma, (ii) high-temperature crustal metamorphism at 4555 Ma, and (iii) subsequent monotonic cooling with a low cooling rate of 11 ± 2 °C/Myr (Iizuka et al., 2019) in the deep crust over the next ~60 Myr.

The merrillite in Ibitira recorded an earlier event, with the model ^{207}Pb*/^{206}Pb* age of 4552.0 ± 8.8 Ma (Fig. 4). This value is indistinguishable from its pyroxene ^{207}Pb–^{206}Pb isochron age of 4556.75 ± 0.57 Ma (Iizuka et al., 2014). The whole-rock Mn–Cr systems also recorded this age (4557 +2/−4 Ma; Lugmair and Shukolyukov, 1998). Thermal metamorphism at ~4555 Ma is consistent with the records in the eucrites, even though Ibitira came from a different parent body. The ^{40}Ar–^{39}Ar age of 4487 ± 15 Ma for Ibitira is distinctly younger than those from the other chronometers (Bogard and Garrison, 1995). It is inferred that Ibitira experienced (i) ancient crystallization likely prior to 4560 Ma, (ii) high-temperature thermal metamorphism in the crust at 4555 Ma, and (iii) subsequent monotonic cooling until ~4490 Ma.

5.4. Intense asteroidal collisions prior to 4.15 Ga?

Our study reveals that the U–Pb system in the phosphates in the three brecciated eucrites recorded multiple impact events prior to 4.15 Ga. The phosphates U–Pb ages of two other brecciated eucrites, NWA 8009 and Béréba, also recorded the thermal events at ~4.25–4.1 Ga (Liao and Hsu, 2017; Zhou et al., 2011). Moreover, the silicate U–Pb systems in some eucrites recorded coincident timings (Galer and Lugmair, 1996; Tera et al., 1997). It is obvious that the parent body, Vesta, suffered intense impacts at ≥4.15 Ga, during which the U–Pb systems in its phosphates and silicates were partially reset. Conversely, only the K–Ar system recorded the later bombardment on Vesta (or the V-type asteroids) at 3.85–3.47 Ga (Kennedy et al., 2019). The absence of ~3.85-Ga records in the phosphates U–Pb systems suggests that these later impacts were weaker than the earlier impacts (>4.15 Ga), resulting in lower reheating temperatures.

The closure temperatures T_c of the U–Pb system in zircon and apatite, and of the K–Ar system in plagioclase are calculated using Dodson's law (Dodson, 1973): $T_c = E/R\ln(ARD_0T_c^2/a^2ET')$, where E = activation energy, R = gas constant, D_0 = diffusion coefficient, and A is a dimensionless constant, with known diffusion properties of Pb and/or Ar (Cherniak and Watson, 2000; Cherniak et al., 1991; Cassata et al., 2009). For diffusion scale (a), we use typical grain sizes of the minerals in the basaltic eucrites. Cooling rate T' is an unknown parameter. In high-temperature range (1200 °C–850 °C), T' for the basaltic eucrites is known to be as rapid as 4000 °C/Myr (Miyamoto and Takeda, 1977). By extrapolating this to the lower temperature range, T_c becomes ~590 °C for the U–Pb in apatite and ~300 °C for the K–Ar in plagioclase. The detailed conditions for the T_c calculations and their results are provided in supplementary Table S3. In case of impact-induced reheating and subsequent rapid quenching at the near-surface of the asteroid the closure temperatures are much higher. Assuming a rapid quenching 1 °C/d (or, 4 × 10^8 °C/Myr) after impact reheating, T_c becomes ~1000 °C for the U–Pb in apatite, ~500 °C for the K–Ar in plagioclase, and exceed the melting point of basaltic rock for the U–Pb in zircon (Supplementary Table S3). This means the U–Pb ages in the eucrite zircon may not be disturbed by impacts without extensive remelting and/or recrystallization, unless our assumption of the rapid quenching is incorrect.

In Fig. 5, we compiled the literature data for the U–Pb and Hf–W chronologies of zircon, the U–Pb system of silicates and phosphates, and the K–Ar system of whole-rock or silicates (dated by the ^{40}Ar-^{39}Ar method) for various basaltic eucrites and mesosiderites. There seem to be three key age groups: (1) prior to 4.5 Ga, (2) prior to 4.15 Ga, and (3) near ~3.9–3.5 Ga.

(1) The initial magmatic crystallization (4.56 Ga) and subsequent thermal metamorphism occurred prior to 4.5 Ga. The U–Pb ages of the various eucrite zircons reveal the timing of the ubiquitous thermal metamorphism of the initial basaltic crust of Vesta to be 4.55 Ga at a metamorphic temperature of ~900 °C (Iizuka et al., 2015). After an intensive initial differentiation at 4.56 Ga, the magmatism on Vesta lasted until 4.53 Ga, according to the Hf–W records of unbrecciated eucrite zircon (Roszjar et al., 2016). In addition, the asteroid may have suffered a large basin-forming collision at this stage (Hopkins et al., 2015; Kennedy et al., 2019). The U-Pb, and Hf–W studies of mesosiderite zircons also provide a high-temperature reheating age of 4.53 Ga (Haba et al., 2017, 2019; Koike et al., 2017) that is attributed to a catastrophic collision.

(2) After this early event 1, the asteroid experienced moderate collisions prior to 4.15 Ga. At this stage, none of the earlier zircon crystals were remelted or recrystallized and the crystals' U–Pb and Hf–W chronologies remained closed. Instead, the impacts were recorded by the U–Pb systems in phosphates (this study; Liao and Hsu, 2017; Zhou et al., 2011) and silicates (Galer and Lugmair, 1996; Tera et al., 1997) in several brecciated eucrites. The reheating temperature likely exceeded their closure temperatures (~590–1000 °C) and rapidly quenched. Some regions may have exceeded the basalt melting point and formed the

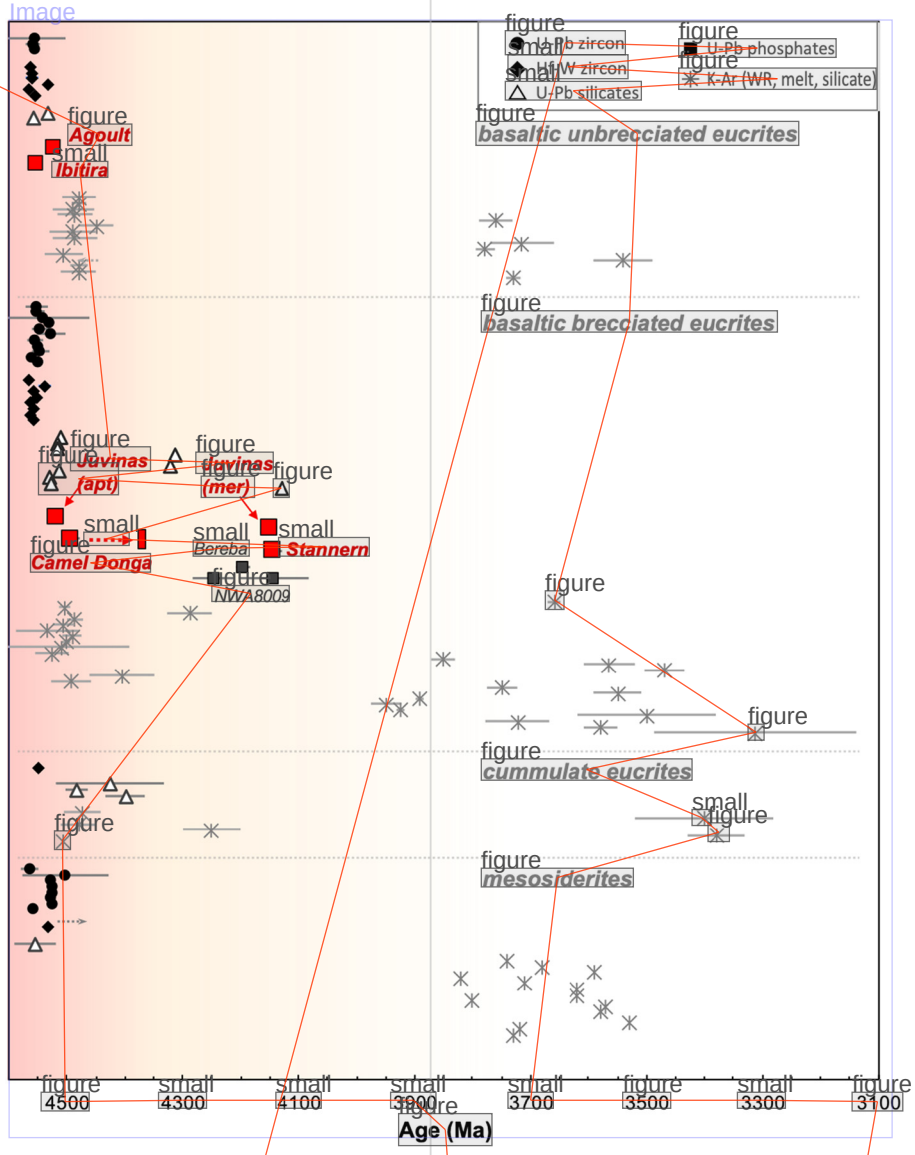

Fig. 5. Compiled chronological data (the U-Pb systems in zircon, silicates, phosphates, the Hf-W system in zircon, and the K-Ar system in whole rock or plagioclase) of basaltic eucrites compared to those of cumulate eucrites and mesosiderites. Our data are depicted by the red-filled symbols. Literature data are from Ireland and Bukovanská (1992), Ireland and Wlotzka (1992), Bukovanska and Ireland (1993), Misawa et al. (2005), Zhou et al. (2013), Iizuka et al. (2015), Haba et al. (2017, 2019) for the U-Pb in zircon; Srinivasan et al. (2007), Roszjar et al. (2016), Koike et al. (2017) for the Hf-W in zircon; Galer and Lugmair (1996), Tera et al. (1997), Iizuka et al. (2014, 2019) for the U-Pb in silicates, Zhou et al. (2011), Liao and Hsu (2017), Liao et al. (2019), and this study for the U-Pb in phosphates; Kaneoka et al. (1995), Bogard and Garrison (2003); Bogard (2011) and references therein, and Kennedy et al. (2013, 2019) for the K-Ar in whole rock, plagioclase, pyroxene, matrix or impact melt.

impact melt. Because the studied eucrites resided at different locations on their parent body, their records indicate multiple collisions during ~4.4–4.15 Ga.

(3) Later collisions occurred at ~3.9–3.5 Ga. These events were recorded only by the ^{40}Ar–^{39}Ar ages, where the reheating temperature may have slightly exceeded the K–Ar closure temperature (~250 °C–500 °C; Table S3). Theoretical calculations indicate that such moderate reheating can be achieved by low-velocity (i.e., slower than the typical relative speed of asteroidal bodies) mild collisions. The absence of a U–Pb record (for either phosphates or silicates) at ~3.9 Ga suggests that these later collisions were much weaker than the earlier ones.

The multiple moderate collisions prior to 4.15 Ga (event 2) could be attributed to the start of the LHB (Liao and Hsu, 2017; Zhou et al., 2011), even though some data in Fig. 5 are significantly earlier than the ^{40}Ar–^{39}Ar ages. Conversely, event 2 can be explained as an "end-tail" of the cataclysmic collisions at the earlier stage of >4.5 Ga (event 1). Such "end-tail" collisions significantly decreased by ~3.9 Ga (event 3), when only weak (or low-velocity) impacts occurred. This interpretation matches the recent theoretical models of an early bombardment (≥4.5 Ga) and a subsequent monotonic decrease in impacts in the inner solar system (Mojzsis et al., 2019; Brasser et al., 2020). Even though the number of key chronological data is still small, this is an important piece of evidence for the early collisional history of the inner solar system. Future studies of other asteroidal materials are expected to help reconstruct the whole history.

6. Conclusions

NanoSIMS U–Pb dating was conducted on apatite and merrillite minerals in three brecciated basaltic eucrites (Juvinas, Camel Donga, and Stannern) and two unbrecciated basaltic achondrites (Agoult and Ibitira). The weighted mean model $^{207}Pb^*/^{206}Pb^*$ age of the Agoult apatite was determined to be 4524.8 ± 9.6 Ma, significantly younger than its zircon age (4555 Ma) and older than the

^{40}Ar–^{39}Ar age of its plagioclase (4496 Ma). This is consistent with a previous interpretation (Iizuka et al., 2015, 2019) that Agoult recorded ubiquitous high-temperature metamorphism of the initial crust of Vesta. The ^{207}Pb*/^{206}Pb* age of the Ibitira merrillite is 4552.0 ± 8.7 Ma, consistent with the other chronometers in this meteorite. Conversely, the model ^{207}Pb*/^{206}Pb* ages of the Juvinas phosphates recorded two distinct events at 4516.9 ± 10.4 Ma (the weighted mean value for apatite) and 4150.3 ± 11.6 Ma (merrillite). The earlier age reflects either crustal metamorphism or an independent impact at ~4520 Ma. The later age reveals the presence of a moderate collisional reheating event at 4150 Ma. This timing is identical to the ^{207}Pb*/^{206}Pb* age of the Stannern apatite and merrillite at 4143.0 ± 12.5 Ma. For the Camel Donga apatite, the model ^{207}Pb*/^{206}Pb* ages present a mean value of 4491.4 ± 13.5 Ma with one exceptionally disturbed value of ~4370 Ma. Apparently, these brecciated eucrites indicate the presence of multiple collisional events during the period of ~4.4–4.15 Ga. By combining our chronological dataset with data from the literature, the thermal and metamorphic history of Vesta's crust can be described as follows: (1) Initial magmatic processes occurred during the period of 4.56–4.5 Ga. Cataclysmic collision(s) also occurred during this stage. (2) The asteroid subsequently experienced multiple collisions during the period of ~4.4–4.15 Ga, which were recorded by the U–Pb systems in apatite, merrillite and some silicates, but not by the U–Pb system in zircons. The reheating temperature exceeded the apatite U–Pb closure temperature (~590–1,000 °C) and likely reached locally the basalt melting point locally. (3) Later collisions at ~3.9–3.5 Ga were recorded only by the K–Ar system. The reheating temperature was likely ≤500 °C, which can be achieved through weak impacts. The records on Vesta are well explained by a scenario with early asteroidal bombardments and a monotonic decrease of the bombardment rate from ≥4.5 Ga to ~4.15 Ga, rather than by the conventional LHB scenario.

CRediT authorship contribution statement

Mizuho Koike: Conceptualization, Funding acquisition, Investigation, Writing - original draft. **Yuji Sano:** Supervision, Writing - review & editing. **Naoto Takahata:** Investigation, Methodology, Writing - review & editing. **Tsuyoshi Iizuka:** Investigation, Writing - review & editing. **Haruka Ono:** Investigation, Writing - review & editing. **Takashi Mikouchi:** Investigation, Writing - review & editing.

Declaration of competing interest

The authors declare that they have no known competing financial interests or personal relationships that could have appeared to influence the work reported in this paper.

Acknowledgements

We are grateful to Dr. F. Moynier for handling this paper. Constructive review comments by Dr. S. J. Mojzsis and Dr. V. Debaille to the former version of this manuscript are sincerely appreciated. The polished section of Stannern eucrite was kindly provided by Dr. M. K. Haba at Tokyo Institute of Technology. We are grateful to Mr. K. Ichimura for assistance with FE-EPMA analyses at the University of Tokyo. The detailed English language was reviewed by Enago (www.enago.jp). This study is partly supported by JSPS Grants-in-Aid for Scientific Research (KAKENHI) to MK (16J07403, 18J02005, and 19K14790), to MK, YS, and TM (19H00726), and by National Institute of Polar Research to HO (NIPR General Collaboration Project no. 28-30).

Appendix A. Supplementary material

Supplementary material related to this article can be found online at https://doi.org/10.1016/j.epsl.2020.116497.

References

Barrat, J.A., Yamaguchi, A., Greenwood, R.C., Bohn, M., Cotton, J., Benoit, M., Franchi, I.A., 2007. The Stannern trend eucrites: contamination of main group eucritic magmas by crustal partial melts. Geochim. Cosmochim. Acta 71, 4108–4124. https://doi.org/10.1016/j.gca.2007.06.001.

Bogard, D.D., 2011. K–Ar ages of meteorites: clues to parent-body thermal histories. Chem. Erde 71, 207–226. https://doi.org/10.1016/j.chemer.2011.03.001.

Bogard, D.D., Garrison, D.H., 1995. ^{39}Ar-^{40}Ar age of the Ibitira eucrite and constraints on the time of pyroxene equilibration. Geochim. Cosmochim. Acta 59, 4317–4322.

Bogard, D.D., Garrison, D.H., 2003. ^{39}Ar-^{40}Ar ages of eucrites and thermal history of asteroid 4 Vesta. Meteorit. Planet. Sci. 38, 669–710.

Brasser, R., Werner, S.C., Mojzsis, S.J., 2020. Impact bombardment chronology of the terrestrial planets from 4.5 Ga to 3.5 Ga. Icarus 338, 113514. https://doi.org/10.1016/j.icarus.2019.113514.

Bukovanska, M., Ireland, T.R., 1993. Zircons in eucrites: pristine and disturbed U-Pb systematics. In: Proc. 56th Annual Meeting of Meteoritical Society. Abstract 333.

Cassata, W.S., Renne, Shuster, D.L., 2009. Argon diffusion in plagioclase and implications for thermochronometry: a case study from the Bushveld Complex, South Africa. Geochim. Cosmochim. Acta 73, 6600–6612. https://doi.org/10.1016/j.gca.2009.07.017.

Cherniak, D.J., Watson, E.B., 2000. Pb diffusion in zircon. Chem. Geol. 172, 5–24. https://doi.org/10.1016/S0009-2541(00)00233-3.

Cherniak, D.J., Lanford, W.A., Ryerson, F.J., 1991. Lead diffusion in apatite and zircon using ion implantation and Rutherford Backscattering techniques. Geochim. Cosmochim. Acta 55, 1662–1673. https://doi.org/10.1016/0016-7037(91)90137-T.

Clement, M.S., Kaib, N.A., Raymond, S.N., Chambers, J.E., Walsh, K.J., 2019. The early instability scenario: terrestrial planet formation during the giant T planet instability, and the effect of collisional fragmentation. Icarus 321, 778–790. https://doi.org/10.1016/j.icarus.2018.12.033.

Dodson, M.H., 1973. Closure temperature in cooling geochronological and petrological systems. Contrib. Mineral. Petrol. 40, 259–274.

Fenner, C.N., 1913. The stability relations of the silica minerals. Am. J. Sci. 36, 331–384.

Galer, S.J.G., Lugmair, G.W., 1996. Lead isotopic systematics of noncumulate eucrites. In: 59th Annual Meeting of Meteoritical Society. Abstract A47.

Gomes, R., Levison, H.F., Tsiganis, K., Morbidelli, A., 2005. Origin of the cataclysmic Late Heavy Bombardment period of the terrestrial planets. Nature 435, 466–469. https://doi.org/10.1038/nature03676.

Greenwood, R.C., Franchi, I.A., Jambon, A., Buchanan, P.C., 2005. Widespread magma oceans on asteroidal bodies in the early Solar System. Nature 435, 916–918.

Haba, M.K., Yamaguchi, A., Horie, K., Hidaka, H., 2014. Major and trace elements of zircons from basaltic eucrites: implications for the formation of zircons on the eucrite parent body. Earth Planet. Sci. Lett. 387, 10–21. https://doi.org/10.1016/j.epsl.2013.11.006.

Haba, M.K., Yamaguchi, A., Kagi, H., Nagao, K., Hidaka, H., 2017. Trace element composition and U-Pb age of zircons from Estherville: constraints on the timing of the metal-silicate mixing event on the mesosiderite parent body. Geochim. Cosmochim. Acta 215, 76–91. https://doi.org/10.1016/j.gca.2017.07.028.

Haba, M.K., Wotzlaw, J-F., Lai, Y-J., Yamaguchi, A., Schönbächler, M., 2019. Mesosiderite formation on asteroid 4 Vesta by a hit-and-run collision. Nat. Geosci. 12, 510–515. https://doi.org/10.1038/s41561-019-0377-8.

Hopkins, M.D., Mojzsis, S.J., Bottke, W.F., Abramov, O., 2015. Micrometer-scale U–Pb age domains in eucrite zircons, impact re-setting, and the thermal history of the HED parent body. Icarus 245, 367–378. https://doi.org/10.1016/j.icarus.2014.08.025.

Hublet, G., Debaille, V., Wimpenny, J., Yin, Q-Z., 2017. Differentiation and magmatic activity in Vesta evidenced by ^{26}Al-^{26}Mg dating in eucrites and diogenites. Geochim. Cosmochim. Acta 218, 73–97. https://doi.org/10.1016/j.gca.2017.09.005.

Iizuka, T., Amelin, Y., Kaltenbach, A., Koefoed, P., Stirling, C.H., 2014. U–Pb systematics of the unique achondrite Ibitira: precise age determination and petrogenetic implications. Geochim. Cosmochim. Acta 132, 259–273.

Iizuka, T., Yamaguchi, A., Haba, M.K., Amelin, Y., Holden, P., Zink, S., Huyskens, M.H., Ireland, T.R., 2015. Timing of global crustal metamorphism on Vesta as revealed by high-precision U–Pb dating and trace element chemistry of eucrite zircon. Earth Planet. Sci. Lett. 409, 182–192.

Iizuka, T., Jourdan, F., Yamaguchi, A., Koefoed, P., Hibiya, Y., Ito, K.T.M., Amelin, Y., 2019. The geologic history of Vesta inferred from combined ^{207}Pb/^{206}Pb and ^{40}Ar/^{39}Ar chronology of basaltic eucrites. Geochim. Cosmochim. Acta 267, 275–299. https://doi.org/10.1016/j.gca.2019.09.034.

Ireland, T.R., Bukovanská, M., 1992. Zircons from the Stannern eucrites. In: Proc. 55th Annual Meeting of Meteoritical Society. Abstract 237.

references
Ireland, T.R., Wlotzka, F., 1992. The oldest zircons in the solar system. Earth Planet. Sci. Lett. 109, 1–10. https://doi.org/10.1016/0012-821X(92)90069-8.

Kaneoka, I., Nagao, K., Yamaguchi, A., Takeda, H., 1995. ^{39}Ar-^{40}Ar analyses of Juvinas fragments. Proc. NIPR Symp. Antarct. Meteor. 8, 287–296.

Kennedy, T., Jourdan, F., Bevan, A.W.R., Gee, M.A.M., Frew, A., 2013. Impact history of the HED parent body(ies) clarified by new ^{40}Ar/^{39}Ar analyses of four HED meteorites and one anomalous basaltic achondrite. Geochim. Cosmochim. Acta 115, 163–183.

Kennedy, T., Jourdan, F., Eroglu, E., Mayers, C., 2019. Bombardment history of asteroid 4 Vesta recorded by brecciated eucrites: large impact event clusters at 4.50 Ga and discreet bombardment until 3.47 Ga. Geochim. Cosmochim. Acta 260, 99–123.

Koike, M., Ota, Y., Sano, Y., Takahata, N., Sugiura, N., 2014. High-spatial resolution U–Pb dating of phosphate minerals in Martian meteorite Allan Hills 84001. Geochem. J. 48, 423–431.

Koike, M., Sugiura, N., Takahata, N., Ishida, A., Sano, Y., 2017. U-Pb and Hf-W dating of young zircon in mesosiderite Asuka 882023. Geophys. Res. Lett. 44, 1251–1259. https://doi.org/10.1002/2016GL071609.

Kunz, J., Trieloff, M., Bobe, K.D., Metzler, K., Stöffler, D., Jessberger, E.K., 1995. The collisional history of the HED parent body inferred from ^{40}Ar-^{39}Ar ages of eucrites. Planet. Space Sci. 43, 527–543.

Liao, S., Hsu, W., 2017. The petrology and chronology of NWA 8009 impact melt breccia: implication for early thermal and impact histories of Vesta. Geochim. Cosmochim. Acta 204, 159–178. https://doi.org/10.1016/j.gca.2017.01.037.

Liao, S., Hsu, W., Wang, Y., Li, Y., Tang, C., Mei, B., 2019. In situ Pb-Pb dating of silica-rich Northwest Africa (NWA) 6594 basaltic eucrite and its constraint on thermal history of the Vestan crust. Meteorit. Planet. Sci. 54, 3064–3081. https://doi.org/10.1111/maps.13408.

Ludwig, K.R., 2012. User's Manual for Isoplot 3.75: A Geochronological Toolkit for Microsoft Excel. Special Publication No. 5. Berkeley Geochronology Center.

Lugmair, G.W., Shukolyukov, A., 1998. Early solar system timescales according to ^{53}Mn-^{53}Cr systematics. Geochim. Cosmochim. Acta 62, 2863–2886.

McCord, T.B., Adams, J.B., Johnson, T.V., 1970. Asteroid Vesta: spectral reflectivity and compositional implications. Science 168, 1445–1447. http://science.sciencemag.org/content/168/3938/1445.

McSween, H.Y., Binzel, R.P., De Sanctis, M.C., Ammannito, E., Prettyman, T.H., Beck, A.W., Reddy, V., Corre, L.L., Gaffey, M.J., McCord, T.B., Raymond, C.A., Russell, C.T., the Dawn Science Team, 2013. Dawn; the Vesta–HED connection; and the geologic context for eucrites, diogenites, and howardites. Meteorit. Planet. Sci. 48, 2090–2104.

Metzler, K., Bobe, K.D., Palme, H., Spettel, B., Stöffler, D., 1995. Thermal and impact metamorphism on the HED parent asteroid. Planet. Space Sci. 43, 499–525.

Misawa, K., Yamaguchi, A., Kaiden, H., 2005. U-Pb and ^{207}Pb-^{206}Pb ages of zircons from basaltic eucrites: implications for early basaltic volcanism on the eucrite parent body. Geochim. Cosmochim. Acta 69, 5847–5861.

Miyamoto, M., Takeda, H., 1977. Evaluation of a crust model of eucrites from the width of exsolved pyroxene. Geochem. J. 11, 161–169.

Miyamoto, M., Mikouchi, T., Kaneda, K., 2001. Thermal history of the Ibitira noncumulate eucrite as inferred from pyroxene exsolution lamella: evidence for reheating and rapid cooling. Meteorit. Planet. Sci. 36, 231–237.

Mojzsis, S.J., Brasser, R., Kelly, N.M., Abramov, O., Werner, S.C., 2019. Onset of Giant planet migration before 4480 million years ago. Astrophys. J. 881, 44. https://doi.org/10.3847/1538-4357/ab2c03.

Morbidelli, A., Nesvorny, D., Laurenz, V., Marchi, S., Rubie, D.C., Elkins-Tanton, L., Wieczorek, M., Jacobson, S., 2018. The timeline of the lunar bombardment: revisited. Icarus 305, 262–276. https://doi.org/10.1016/j.icarus.2017.12.046.

Neumann, W., Breuer, D., Spohn, T., 2014. Differentiation of Vesta: implications for a shallow magma ocean. Earth Planet. Sci. Lett. 395, 267–280.

Ono, H., Mikouchi, T., Yasutake, M., Takenouchi, A., Koike, M., Iizuka, T., Yamaguchi, A., Miyake, A., Tsuchiyama, A., 2018. Silica minerals and pyroxenes in the Camel Donga non-cumulate eucrite: further evidence for its polymict nature. Proc. NIPR Symp. Antarct. http://id.nii.ac.jp/1291/00015143.

Palme, H., Wlotzka, F., Spettel, B., Dreibus, G., Weber, H., 1988. Camel Donga: a eucrite with high metal content. Meteoritics 23, 49–57.

Roszjar, J., Whitehouse, M.J., Srinivasan, G., Mezger, K., Scherer, E.E., Van Orman, J.A., Bischoff, A., 2016. Prolonged magmatism on 4 Vesta inferred from Hf–W analyses of eucrite zircon. Earth Planet. Sci. Lett. 452, 216–226.

Russell, C.T., Raymond, C.A., Coradini, A., McSween, H.Y., Zuber, M.T., Nathues, A., De Sanctis, M.C., Jaumann, R., Konopliv, A.S., Preusker, F., Asmar, S.W., Park, R.S., Gaskell, R., Keller, H.U., Mottola, S., Roatsch, T., Scully, J.E.C., Smith, D.E., Tricarico, P., Toplis, M.J., Christensen, U.R., Feldman, W.C., Lawrence, D.J., McCoy, T.J., Prettyman, T.H., Reedy, R.C., Sykes, M.E., Titus, T.N., 2012. Dawn at Vesta: testing the protoplanetary paradigm. Science 336, 684–686. http://science.sciencemag.org/content/336/6082/684.

Sano, Y., Oyama, T., Terada, K., Hidaka, H., 1999. Ion microprobe U–Pb dating of apatite. Chem. Geol. 153, 249–258.

Sano, Y., Terada, K., Takeno, S., Taylor, L., McSween, H.Y., 2000. Ion microprobe uranium-thorium-lead dating of Shergotty phosphates. Meteorit. Planet. Sci. 35, 944–946.

Scott, E.R.D., Greenwood, R.C., Franchi, I.A., Sanders, I.S., 2009. Oxygen isotopic constraints on the origin and parent bodies of eucrites, diogenites, and howardites. Geochim. Cosmochim. Acta 73, 5835–5853.

Srinivasan, G., Whitehouse, M.J., Weber, I., Yamaguchi, A., 2007. The crystallization age of eucrite zircon. Science 317, 345–347. http://www.sciencemag.org/content/317/5836/345.full.html.

Stöffler, D., Ryder, G., 2001. Stratigraphy and isotope ages of lunar geologic units: chronological standard for the inner solar system. In: Kallenbach, R., Geiss, J., Hartmann, W. (Eds.), Chronology and Evolution of Mars. Springer, Netherlands, Dordrecht, pp. 9–54. https://link.springer.com/chapter/10.1007/978-94-017-1035-0_2.

Takahata, N., Tsutsumi, Y., Sano, Y., 2008. Ion microprobe U–Pb dating of zircon with a 15 micrometer spatial resolution using NanoSIMS. Gondwana Res. 14, 587–596. https://doi.org/10.1016/j.gr.2008.01.007.

Takeda, H., Graham, A.L., 1991. Degree of equilibration of eucritic pyroxenes and thermal metamorphism of the earliest planetary crust. Meteoritics 26, 129–134.

Tera, F., Carlson, R.W., Boctor, N.Z., 1997. Radiometric ages of basaltic achondrites and their relation to the early history of the Solar System. Geochim. Cosmochim. Acta 61, 1713–1731.

Terada, K., Sano, Y., 2002. Ion microprobe U-Pb dating and REE analyses of phosphates in H4-chondrite, Yamato-74371. Geophys. Res. Lett. 29, 98. https://doi.org/10.1029/2001GL01394.

Touboul, M., Sprung, P., Aciego, S.M., Bourdon, B., Kleine, T., 2015. Hf–W chronology of the eucrite parent body. Geochim. Cosmochim. Acta 156, 106–121.

Turner, G., Cadogan, P.H., Young, C.J., 1973. Apollo 17 age determinations. Nature 242, 513–515.

Warren, P.H., Isa, J., Ebihara, M., Yamaguchi, A., Baecker, B., 2017. Secondary-volatiles linked metallic iron in eucrites: the dual-origin metals of Camel Donga. Meteorit. Planet. Sci. 52, 737–761.

Yamaguchi, A., Taylor, G.J., Keil, K., 1996. Three unbrecciated equilibrated eucrites: global metamorphism on the eucrite parent body. In: Proc. 27th Lunar Planet. Sci. Conf. Abstract 1469.

Yamaguchi, A., Barrat, J.A., Greenwood, R.C., Shirai, N., Okamoto, C., Setoyanagi, T., Ebihara, M., Franchi, I.A., Bohn, M., 2009. Crustal partial melting on Vesta: evidence from highly metamorphosed eucrites. Geochim. Cosmochim. Acta 73, 7162–7182.

Zhou, Q., Yin, Q.-Z., Bottoke, B., Claeys, P. Li, X.-H., Wu, F.-Y., Li, Q.-L., Liu, Y., Tang, G.-Q., 2011. Early basaltic volcanism and late heavy bombardment on Vesta: U-Pb ages of small zircons and phosphates in eucrites. In: Proc. 42nd Lunar and Planet. Sci. Conf. Abstract 2575.

Zhou, Q., Yin, Q.-Z., Young, E.D., Li, X.-H., Wu, F.-Y., Li, Q.-L., Liu, Y., Tang, G.-Q., 2013. SIMS Pb–Pb and U–Pb age determination of eucrite zircons at <5 μm scale and the first 50 Ma of the thermal history of Vesta. Geochim. Cosmochim. Acta 110, 152–175.